HHS Public Access

Author manuscript

Nat Med. Author manuscript; available in PMC 2012 July 01.

Published in final edited form as:

Nat Med. ; 18(1): 111–119. doi:10.1038/nm.2550.

Reversible cell cycle entry in adult kidney podocytes through regulated control of telomerase and Wnt signaling

Marina Shkreli[1,2], **Kavita Y. Sarin**[1], **Matthew F. Pech**[1,3], **Natalia Papeta**[4], **Woody Chang**[1], **Stephanie A. Brockman**[1], **Peggie Cheung**[1], **Eunice Lee**[1], **Frank Kuhnert**[1], **Jean L. Olson**[5], **Calvin J. Kuo**[1,3], **Ali G. Gharavi**[4], **Vivette D. D'Agati**[6], and **Steven E. Artandi**[1,3,7]

[1]Department of Medicine, Stanford School of Medicine, Stanford, CA 94305

[3]Program in Cancer Biology, Stanford School of Medicine, Stanford, CA 94305

[4]Department of Medicine, Columbia University, New York, NY 10032

[5]Department of Pathology, UCSF, San Francisco, CA 94143

[6]Department of Pathology, Columbia University, New York, NY 10032

[7]The Glenn Laboratories for the Biology of Aging, Stanford University School of Medicine, Stanford, CA 94305, USA

Abstract

Mechanisms of epithelial cell renewal remain poorly understood in the mammalian kidney, particularly in the glomerulus, a site of cellular damage in chronic kidney disease. Within the glomerulus, podocytes – differentiated epithelial cells critical for filtration – are thought to lack significant capacity for regeneration. Here, we show that podocytes rapidly lose differentiation markers and enter cell cycle in adult mice in which the telomerase protein component TERT is conditionally expressed. Transgenic TERT expression induces marked upregulation of Wnt signaling and disrupts glomerular structure resulting in a collapsing glomerulopathy resembling those in humans, including HIV-associated nephropathy (HIVAN). Human and mouse HIVAN kidneys show increased levels of TERT and activation of Wnt signaling, indicating that these are general features of collapsing glomerulopathies. Either silencing transgenic TERT expression or inhibition of Wnt signaling through systemic expression of the Wnt-inhibitor Dkk1 in TERT transgenic mice results in marked normalization of podocytes, including rapid cell cycle exit, re-expression of differentiation markers and improved filtration barrier function. These data reveal an unexpected property of podocytes to reversibly enter cell cycle, suggest that podocyte renewal may contribute to glomerular homeostasis and implicate the telomerase and Wnt/β-catenin pathways in podocyte proliferation and disease.

Correspondence to: Steven E. Artandi.

[2]Current address: Laboratory of Biology and Pathology of Genomes, University of Nice, Nice, France

Author Contributions M.S., K.Y.S., M.F.P., N.P., F.K., J.L.O., C.J.K., A.G.G., V.D.A and S.E.A. designed the experiments and analyzed data; M.S., K.Y.S., M.F.P., N.P., F.K., W.C., S.A.B., P.C., and E.L. performed the experiments; and M.S. and S.E.A. wrote the manuscript.

Keywords

kidney; podocyte; glomerulus; collapsing glomerulopathy; telomerase; TERT; Wnt

INTRODUCTION

Kidney epithelium serves a remarkable array of structural and metabolic functions in guiding the formation and processing of a plasma filtrate into urine. Numerous disease processes, drugs and toxins target kidney epithelium, highlighting the need to understand mechanisms of kidney cell renewal in health and in disease. Under steady-state, unstressed conditions, epithelial turnover in the kidney occurs at a slow rate[1]. However, damage to the kidney tubules results in a brisk regenerative response, whereby lost cells are replenished from a source intrinsic to the tubular epithelium[2]. In contrast, less is known regarding mechanisms of renewal of epithelial cells within the glomerulus, a complex structure containing capillary loops and multiple cell types that together serve as the kidney filtration unit. Within the glomerulus, podocytes – visceral epithelial cells crucial for effective filtration – are damaged or reduced in number in 90% of chronic kidney diseases in humans[3].

Depletion of podocytes and the inability to repopulate a damaged glomerulus with functional podocytes ultimately leads to glomerulosclerosis, or scarring of the glomerulus[4,5]. Diabetes and other systemic disease states can initiate these changes in podocytes, which in turn can result in end-stage renal failure[6,7]. Podocytes are differentiated cells whose foot processes cover the basement membrane of the glomerulus and form the filtration slit diaphragms controlling blood filtration[8]. Mature podocytes do not express proliferation markers, and these observations together with their minimal ability to respond to injury suggested that podocytes have a limited capacity to proliferate or renew during life[9,10]. Despite these observations, podocyte proliferation does occur in the rare collapsing variant of focal segmental glomerulosclerosis (FSGS), suggesting that podocytes possess proliferative potential. In two collapsing glomerulopathies, one an idiopathic form of unknown etiology and the other caused by human immunodeficiency virus (HIV), podocyte dedifferentiation and cell cycle entry compromise the filtration barrier, leading to severe organ damage[11]. Results from transgenic mouse models of HIV-associated nephropathy (HIVAN) implicated the HIV-1 open reading frames nef and vpr as contributors to HIVAN pathogenesis[12–14]. Cellular pathways involved in the control of the proliferative state of podocytes include VEGF and Vhlh[15,16]. Recent evidence suggests that the parietal cell layer lining Bowman's capsule may provide a niche for cells able to repopulate depleted podocytes in humans and in mice[17,18]. However, little is known about the cellular pathways that govern podocyte renewal during life and whether proliferating podocytes can attain a differentiated phenotype.

One pathway important for tissue renewal involves telomerase, an enzyme complex in tissue progenitor cells and cancers that synthesizes telomere repeats, thereby preventing telomere dysfunction, which impairs progenitor cell survival and stem cell self-renewal[19–21]. Telomere maintenance by telomerase requires both components of the catalytic core of the

enzyme: TERT, the telomerase reverse transcriptase, and TERC, the telomerase RNA component, which encodes the template for telomere addition. In addition to its role in telomere maintenance, TERT can act as a co-factor to modulate transcriptional responses controlled by the Wnt signaling pathway. Conditional overexpression of TERT in mouse skin activated hair follicle bulge stem cells, promoting the active phase of the hair follicle cycle and hair growth. The ability of TERT to activate bulge stem cells was independent of TERC and of catalytic function, indicating that it operated through a discrete developmental pathway[22,23]. TERT executes this stem cell activation program by interacting with the chromatin remodeling protein Brg1, at target gene chromatin, including the promoter of the c-Myc gene[24]. Here we report that conditional overexpression of TERT in adult mouse kidney triggers a potent and reversible proliferative response in podocytes by activating the Wnt signaling pathway. Our data demonstrate the capacity of mature podocytes to reversibly enter cell cycle and suggest that the telomerase and Wnt pathways are important in podocyte proliferation and in podocyte disease states.

RESULTS

TERT expression in kidney induces a collapsing glomerulopathy

To determine the effects of TERT on epithelial tissues, we studied doxycycline-inducible TERT (i-TERT) mice, generated by intercrossing tetop-TERT+ and β-actin-rtTA+ transgenic strains[22]. Mice were weaned at three weeks of age, and treated with doxycycline drinking water to induce TERT expression. TERT overexpression was induced broadly in adult tissues (Fig. S1a,b). By age three months, many i-TERT mice on doxycycline became moribund and developed abdominal distension caused by ascites, whereas all control mice remained healthy (median survival 115 days, $P<0.001$)(Fig. 1a). Liver function tests were normal and histology of liver and heart were not significantly changed (Fig. S1c, and data not shown). In contrast, kidneys from i-TERT mice on doxycycline showed dilated microcystic tubules (Fig. 1b) and markedly abnormal glomeruli with wrinkling and retraction of glomerular basement membranes, enlarged, vacuolated podocytes and prominent glomerular epithelial cell hyperplasia (Fig. 1c, d). These features are characteristic of the collapsing variant of FSGS in humans[25] and were seen only in i-TERT mice on doxycycline, but never in i-TERT mice off doxycycline or in single transgenic mice treated with doxycycline, indicating that the phenotype is specifically caused by TERT expression (Fig. 1c,e) (Table S1).

To understand whether these effects on glomerular histology required the catalytic function of TERT in elongating telomeres, we pursued two complementary strategies. First, we disrupted the telomerase catalytic core by expressing TERT in the absence of Terc. Overexpression of TERT resulted in indistinguishable collapsing glomerulopathies in $Terc^{+/+}$, $Terc^{+/-}$ and $Terc^{-/-}$ backgrounds, indicating that TERT can function independently of Terc in this context (Fig. 1e) (Table S2). Second, we employed an inducible TERT allele ($TERT^{ci}$) rendered catalytically inactive through introduction of a point mutation in the active site of the reverse transcriptase domain[23]. Kidneys from i-$TERT^{ci}$ mice showed a collapsing glomerulopathy similar to that seen in i-TERT mice (Fig. 1e) (Table S1). Together, these findings indicate that TERT induces a collapsing

glomerulopathy through a mechanism that does not require catalytic function, instead implicating TERT's non-canonical role as a transcriptional coactivator.

TERT promotes podocyte proliferation and de-differentiation

To characterize the nature of the glomerular abnormalities caused by TERT expression, we studied TERT expression patterns in wild-type and transgenic kidney. In wild-type mice, telomerase activity by TRAP and TERT mRNA by qRT-PCR were both readily detected in newborn kidney but diminished by age 21 days, paralleling the period of postnatal glomerulogenesis (Fig. 1f,g). Whereas telomerase was expressed at very low or undetectable levels in kidneys from adult wild-type mice, transgenic TERT mRNA was specifically upregulated in kidneys from i-TERT mice on doxycycline by Northern blot (Fig. 1h). The β-actin element used to direct expression of rtTA in this model was previously shown to be preferentially active within the kidney in podocytes[26], reflecting the importance of the actin cytoskeleton in podocyte function[27]. Consistent with these previous reports, we found that transgenic TERT mRNA was enriched in podocytes in i-TERT and i-TERT^{ci} mice on doxycycline by RNA in situ hybridization (Fig. 1i, Fig. S2a). To survey podocyte function, we analyzed urine by SDS-PAGE, revealing the presence of abundant albumin in the urine of i-TERT mice on doxycycline (Fig. 1j). These data indicate that TERT is induced in podocytes of i-TERT mice, compromising the ability of these cells to support their normal filtration function.

Podocytes are differentiated and arrested in the G0 phase of the cell cycle[28,29]. To understand how podocytes are altered by TERT overexpression, we assessed proliferation and differentiation in kidneys from i-TERT mice and controls. Glomeruli from i-TERT and i-TERT^{ci} mice showed a marked increase in the abundance of cells positive for the proliferation marker Ki-67, whereas Ki-67+ cells were rare in controls (Fig.2a,b). These proliferative cells were in positions consistent with both podocytes and parietal epithelial cells lining Bowman's capsule (Fig. 2a). Proliferating cells incorporated BrdU indicating progression through S-phase of the cell cycle (Fig. S2b). To study cellular differentiation, we analyzed expression of WT1, a transcription factor that marks mature podocytes[30], and synaptopodin, an actin-associated protein that contributes to foot process formation in differentiated podocytes[31]. Podocytes in i-TERT and i-TERT^{ci} mice on doxycycline showed a profound loss of the podocyte differentiation markers WT1 and synaptopodin (Fig. 2c–e). To understand the relationship between loss of podocyte differentiation markers and the appearance of proliferating cells, groups of i-TERT^{ci} mice were sacrificed between 7 days and 30 days of doxycyline-treatment. Loss of synaptopodin expression was evident at the earliest time point (7 days) and WT1 expression was lost more gradually (Fig. 2f, Fig. S2c). Cell proliferation in glomeruli correlated with WT1 downregulation, reaching a maximum at 12 days with 82% of glomeruli harboring Ki-67 positive cells in i-TERT^{ci} mice (Fig. 2f). Apoptotic cells were not identified (Fig. S2d). Proteinuria by SDS-PAGE was first detected at day 5 and worsened substantially over time (Fig. 2g).

To definitively assess whether proliferating cells in the glomerulus included podocytes, double stains for WT1 and Ki-67 were performed. Double positive WT1+ Ki-67+ cells were rare, but were detected in samples from day 12 of the time course, a period in which both

WT1+ and Ki-67+ cells co-existed (Fig. 2h). Moreover, mitotic figures were evident in podocytes in tissue sections from i-TERT mice (Fig. 2i). Electron microscopy showed enlargement of podocytes and effacement of foot processes in i-TERT^{ci} mice on doxycycline (Fig. 2j, right), but preservation of foot processes in control mice on doxycycline (Fig. 2j, left). In addition, podocytes of i-TERT^{ci} mice on doxycycline show dilated rough endoplasmic reticulum filled with proteinaceous material, consistent with metabolic activation of these cells (Fig. S2e, right). Altogether, these data indicate that TERT induces proliferation of podocytes and that podocytes enter the cell cycle concomitant with downregulation of WT1.

Activation of the Wnt signaling pathway in podocytes

Based on our previous studies linking telomerase to the Wnt program [22–24], we hypothesized that activation of Wnt signaling may underlie podocyte activation in i-TERT mice. To interrogate the Wnt pathway, we performed immunostaining for β-catenin in kidney sections from i-TERT^{ci} mice. Membranous β-catenin was weakly detected in wild-type podocytes in adherens junctions[32,33]. In contrast, β-catenin was strongly upregulated in glomeruli of i-TERT^{ci} mice, in a membranous and cytoplasmic pattern, as well as in the nucleus (Fig.3a). Cells with increased β-catenin were positive for BrdU, indicating that β-catenin is upregulated in proliferating podocytes (Fig. 3b). To understand the timing of β-catenin upregulation in this model, we analyzed kidneys from i-TERT^{ci} mice at 12 days after doxycycline treatment, an early time point at which WT1 is still detectable in many glomeruli. At this early time point, cells with high β-catenin expression were also positive for WT1 in i-TERT^{ci} mice on doxycycline (Fig. 3c). WT1 signal was reduced in these cells compared to wild-type control, indicating that β-catenin upregulation occurs during de-differentiation and loss of WT1 and that β-catenin remains elevated once podocytes enter cell cycle.

To more directly query the Wnt pathway at the transcriptional level, we employed a reporter strain in which lacZ was knocked-in to the endogenous *Axin2* gene, a robust target of Wnt signaling[34]. Compound i-TERT^{ci}; *Axin2*$^{LacZ/+}$ mice were treated with doxycycline for 13 days and kidneys were stained with X-gal. In control Actin-rtTA+; *Axin2*$^{LacZ/+}$ mice on doxycycline, β-galactosidase expression was detected in the renal pelvis, with weaker staining in the medulla and cortex. In contrast, β-galactosidase expression was markedly increased in the medulla and cortex, but diminished in the renal pelvis in i-TERT^{ci}; *Axin2*$^{LacZ/+}$ mice on doxycycline (Fig. 3d). Analysis of kidney whole mounts showed a pattern consistent with increased β-galactosidase activity within glomeruli in i-TERT^{ci}; *Axin2*$^{LacZ/+}$ mice on doxycycline (Fig. 3d, arrows). Indeed, immunostaining revealed a specific increase in β-galactosidase protein within glomeruli of i-TERT^{ci}; *Axin2*$^{LacZ/+}$ mice on doxycycline compared to controls (Fig. 3e, Fig. S3a). Furthermore, qRT-PCR analysis showed a significant upregulation of the Wnt target genes *Axin2*, *cyclin D2* and *Lef1* in i-TERT^{ci} mice on doxycycline (Fig. 3f). Together, these results show that the Wnt signaling is activated in proliferating podocytes in i-TERT^{ci} mice.

Increased TERT and Wnt signaling in collapsing glomerulopathies

To determine whether TERT upregulation is a feature of collapsing glomerulopathies, TERT mRNA levels were assessed in kidney samples from humans with HIVAN or with idiopathic collapsing glomerulopathy (ICG), and in kidneys from a mouse HIVAN model (Tg26 mice) driven by the HIV genome minus the *gag* and *pol* open reading frames[14,35,36]. In human samples, TERT mRNA was specifically elevated in whole kidney biopsy specimens from individuals with HIVAN compared to healthy controls (Fig. 4a). TERT expression and telomerase activity were also upregulated in kidneys from Tg26 mice compared to non-transgenic controls (Fig. 4b,c). Thus, TERT is commonly upregulated in collapsing glomerulopathies in human and mouse.

To understand whether β-catenin stabilization is a feature of collapsing glomerulopathies, we analyzed β-catenin levels by immunofluorescence in the same samples. In the Tg26 mouse model for HIVAN, we found that β-catenin was strongly upregulated in a membranous and cytoplasmic pattern, as well as within the nucleus, of cells in positions within the glomerulus consistent with podocytes (Fig. 4d, Fig. S3b,c). Co-staining with Ki-67 revealed that β-catenin was elevated in proliferating podocytes, indicating that in both i-TERT^{ci} mice and a mouse model of HIVAN podocyte proliferation is accompanied by marked stabilization of β-catenin (Fig. 4e). Increased levels of activated β-catenin in both i-TERT^{ci} and Tg26 mice was further confirmed by western blot analysis for the activated, unphosphorylated form of β-catenin (Fig. 4f). In normal human kidneys and in classic FSGS, faint β-catenin staining was detected in glomeruli, consistent with low level expression in podocyte adherens junctions (Fig. 4h). In contrast, a marked upregulation of total β-catenin was seen in glomeruli from individuals with HIVAN or ICG (Fig. 4h–j). Double immunostaining revealed that many of the cells with stabilized β-catenin were positive for Ki-67 (Fig. S3d). Quantification of glomeruli carrying stabilized β-catenin showed a similar pattern for either human HIVAN or ICG, with 32% and 28% of glomeruli respectively, showing a high β-catenin signal (Fig. 4g, Fig. S3e). This percentage of glomeruli with highβ-catenin was similar to the percentage of glomeruli with Ki-67 positive cells in individuals with HIVAN or ICG (Fig. 4g). Confocal imaging of human HIVAN and ICG revealed podocytes with prominent cytoplasmic and nuclear β-catenin, a hallmark of cells with active Wnt signaling (Fig. 4i,j). Taken together, these data show that TERT upregulation and β-catenin stabilization are common features of collapsing glomerulopathies and suggest that Wnt activation may be necessary for podocyte proliferation in mouse models and in human disease.

Reversibility of the proliferating podocyte phenotype

Although podocytes proliferate in collapsing glomerulopathies and in i-TERTmice, whether these proliferating cells retain the ability to exit the cell cycle, re-differentiate and resume normal function is unknown. To address this question, six i-TERT^{ci} mice were treated with doxycycline for 13 days, at which point three were sacrificed and the remaining three mice were switched to normal drinking water and aged until at least day 42 (reversed mice) (Fig. 5a, left). The severe proteinuria that developed on doxycycline improved in all three reversed mice and was nearly eliminated in 2 of 3 i-TERT^{ci} mice within 15 days after doxycycline withdrawal (Fig. 5b). Whereas all three i-TERT^{ci} mice sacrificed after 13 days

of doxycycline treatment showed marked podocyte de-differentiation and abundant proliferating podocytes, reversed i-TERT^{ci} mice analyzed 29 days after withdrawal of doxycycline exhibited a pronounced normalization of podocytes. Podocytes showed re-expression of WT1 and synaptopodin and proliferating cells within glomeruli were rare (Fig. 5c,d). Ninety-percent of glomeruli in reversed i-TERT^{ci} mice were WT1+, whereas only 26% of glomeruli expressed WT1 in i-TERT^{ci} mice sacrificed immediately after 13 days of doxycycline (Fig. S4a).

To follow the state of podocytes within a single animal during doxycycline treatment and after doxycycline withdrawal, we performed survival nephrectomy experiments. After 25 days of doxycycline treatment, two i-TERT^{ci} mice and two Actin-rtTA+ mice were subjected to unilateral nephrectomy, then switched to normal drinking water and sacrificed after an additional 21 days (Fig. 5a, right). Whereas “pre-reversal” kidneys exhibited podocyte de-differentiation and cell cycle entry (Fig. 5e,f, left), “post-reversal” kidneys showed a marked normalization of podocytes, with a prominent reduction in podocyte proliferation and an increase in podocyte differentiation (Fig. 5e,f, right). The expression of WT1 increased from 27% of glomeruli in the “pre-reversal” sample to 64% in the “post-reversal” sample (Fig. S4b). The lower frequency of WT1 positive glomeruli (64%) in this doxycycline withdrawal experiment compared with the previous reversal experiment that did not incorporate surgery (90%) may reflect the longer duration of doxycycline treatment or the additional hemodynamic and filtration stress on a single kidney in the nephrectomy setting. Histological analysis mirrored the WT1 staining results in reversed i-TERT^{ci} samples, with 61% of glomeruli showing normal morphology and the remaining 39% displaying abnormalities more similar to classical FSGS, including discrete segmental or global lesions of sclerosis and hyalinosis (Fig. 5g). Podocyte density after reversal and recovery in i-TERT^{ci} mice was indistinguishable from controls (Fig. 5h). Taken together, these data indicate that the marked de-differentiation and proliferation of podocytes caused by TERT expression are strikingly reversible after TERT is extinguished, enabling a significant improvement in podocyte function.

Inhibition of Wnt signaling ameliorates disease progression

To assess the requirement for Wnt activation in disease maintenance and progression in our model, we targeted the Wnt/β-catenin pathway by intravenously injecting an adenovirus encoding the Wnt antagonist Dickkopf-1 (Dkk1), a secreted protein that blocks Wnt signaling at the level of the Wnt coreceptor LRP5/6[37–40]. Adenovirus Dkk1 (Ad-Dkk1) treatment of adult mice results in systemic expression of Dkk1 and was previously shown to rapidly inhibit canonical Wnt signaling in intestinal epithelial cells[41]. Intravenous (IV) injection of either Ad-Dkk1, or a control adenovirus expressing an Immunoglobulin Fc fragment (Ad-Fc) was performed on i-TERT^{ci} mice treated with doxycycline for 14 days (Fig. 6a). The three i-TERT^{ci} mice with the most advanced proteinuria at day 14 were assigned to the Dkk1-treatment group, with the remaining mice treated with Ad-Fc in a control arm. Dkk1 effectively inhibited Wnt signaling in the Ad-Dkk1 group, leading to complete effacement of the glandular architecture of the colon, when compared to normal Ad-Fc injected controls (Fig. S4c).

Proteinuria worsened in an unabated fashion during the time course in mice treated with Ad-Fc (Fig. S4d,e). In contrast, expression of Ad-Dkk1 in i-TERT^{ci} mice caused a marked reduction in proteinuria within 5–8 days of the injection, indicating a substantial improvement in filtration barrier function (Fig. 6b, Fig. S4e). Improved podocyte function was specifically due to Dkk1 expression, because proteinuria never diminished in untreated i-TERT mice maintained on doxycycline for up to 56 days (Fig. S5a), and because both podocyte proliferation and de-differentiation were unabated in i-TERT and i-TERT^{ci} mice as long as TERT expression was maintained (Fig, S5b–d). A detailed analysis of the status of podocytes in the Ad-Dkk1 group revealed a striking normalization of podocytes, with an increase in podocyte differentiation (Fig. 6c, Fig. S4f) and a significant reduction in podocyte proliferation (**Fi**g. 6d, Fig. S4g).

To evaluate the importance of Wnt signaling in the mouse HIVAN model, IV injection of either Ad-Dkk1 or Ad-Fc was performed on 5 to 8 week old Tg26 mice, and animals were analyzed after 9 days. Tubular dilatation and glomerular histology were markedly improved in Tg26 mice injected with Ad-Dkk1 compared with Tg26 mice injected with Ad-Fc (Fig. 6e). Podocyte hyperplasia and the percentage of collapsed glomeruli were significantly diminished in the Ad-Dkk1-injected Tg26 mice compared to the Ad-Fc controls (Fig. 6f,g). The percentage of glomeruli showing segmental or global glomerulosclerosis was not significantly decreased in Dkk1 versus the Fc group, suggesting that Wnt inhibition has little effect on glomeruli that reached an advanced stage of injury and scarring at the time of injection (Fig. 6g). Immunohistochemistry analysis showed a significant increase in podocyte differentiation (Fig. 6h, Fig. S6a), together with a reduced percentage of glomeruli with proliferating cells (Fig. 6i, Fig. S6b), comparing Tg26 mice injected with Ad-Dkk1 versus Ad-Fc. Proteinuria was reduced by day 9 in the Ad-Dkk1 group, although most mice remained proteinuric perhaps due to the prevalence of scarring within the glomerulus in the Tg26 model (Fig. S6c). Assessment of proteinuria at later time points was not possible because of the deleterious effects of systemic Wnt inhibition on the gastrointestinal tract[41]. Taken together, these results show a striking normalization of podocytes upon Wnt pathway inhibition in both i-TERT^{ci} and Tg26 models and suggest new avenues for the development of therapeutic strategies to ameliorate disease in patients with the collapsing variant of FSGS.

DISCUSSION

Although kidney podocytes are thought to lack significant regenerative capacity, we find that podocytes possess the ability to de-differentiate and enter cell cycle in i-TERT mice, and then to revert to their original state and resume their role in supporting filtration after TERT expression is silenced or when Wnt signaling is inhibited. Wnt signals are important for kidney development [42–44] and have been implicated in the repair of damaged kidney tubules [45,46]. Wnt signaling was also shown to contribute to podocyte dysfunction in a mouse model of classical FSGS, in which adriamycin treatment causes podocyte damage, but results in neither podocyte de-differentiation nor proliferation[47,48]. Furthermore, nuclear β-catenin was detected in podocytes in human classical FSGS samples[47]. The common activation of Wnt signaling in classical FSGS on one hand and in i-TERT mice and in HIVAN on another, indicates that Wnt signaling can result in fundamental differences in

podocyte phenotype depending on context. The more dramatic podocyte phenotype in the i-TERT model and other collapsing glomerulopathies, compared with classical FSGS, may relate to differences in TERT levels, the strength of the Wnt signal or to the expression of other cellular or viral cofactors. In the i-TERT model, persistent podocyte proliferation depends upon continued expression of TERT and active Wnt signaling, indicating that these two pathways collaborate to enforce the proliferating podocyte phenotype. Consistent with this hypothesis, enforced expression of activated β-catenin alone in the podocyte lineage leads to early glomerular basement membrane alterations, but is insufficient to induce the collapsing form of FSGS[49]. Our data suggest that TERT upregulation and Wnt activation in collapsing glomerulopathies may reflect a reactivation of these regenerative pathways to an extent not seen in FSGS, perhaps reflecting an earlier stage of podocyte development.

In normal mice and humans, podocytes are quiescent, express high levels of CDK inhibitors and are differentiated, suggesting the possibility that these cells may lack the ability to renew during life. Our findings challenge this idea and suggest the possibility that podocytes, like other epithelial cells, possess regenerative potential. The strikingly reversible nature of podocyte cycling seen in i-TERTmice may reflect a normal program of renewal that occurs throughout life as damaged podocytes need to be replenished. Because of the complex anatomy of the glomerulus and the structural function served by podocytes on the basement membrane, renewing podocytes may be rare and therefore elude easy detection. In the i-TERT model, HIVAN or perhaps even in wild-type mice with injury or with advancing age, podocytes may renew either through a cell duplication mechanism, whereby podocytes enter cycle to yield new daughter cells, or through a facultative stem cell model. The recent finding of putative progenitor cells within the parietal epithelial layer of Bowman's capsule capable of regenerating podocytes is also consistent with replenishment of podocytes under certain conditions [17,18,50].

We speculate that the podocyte depletion seen in many forms of glomerulosclerosis may occur because disease processes fail to activate, interfere with or exhaust podocyte renewal. In this case, drugs that activate telomerase or Wnt signaling may improve glomerular function. Conversely, in collapsing glomerulopathies, where podocytes are hyper-proliferative, telomerase inhibitors or Wnt inhibitors may cause podocyte differentiation, as we have shown with TERT withdrawal and with the use of systemic Dkk1, leading to stabilization of glomerular structure and improved glomerular function. Our data indicate that the telomerase and Wnt pathways are critical in podocyte biology and suggest novel therapeutic strategies to enhance podocyte regeneration, differentiation and repair in glomerular disease.

MATERIAL AND METHODS

Generation of transgenic mice

Tetracycline-regulated i-TERT and i-TERT^{ci} transgenic mice were generated as previously described[22,23]. Mice were PCR genotyped using the following oligonucleotide pairs: GTGCTGGTTGTTGTGCTGTC, GGCGAGTTTACGGGTTGT (actin-rtTA), GCTGGCTGCTCATTCTGTCATCTAC, TAAAAAACCTCCCACACCTCCCCC (tetop-TERT) and GGATGTACTTTGTTAAGGCAGCA, ACAACGGAGTTCCTCAGTGC

(tetop-TERT^{ci}). To study the requirement for Terc, *Terc*$^{+/-}$mice were backcrossed to the FVB/N strain for six generations, then intercrossed with the i-TERT alleles to yield i-TERT mice on *Terc*$^{+/+}$, *Terc*$^{+/-}$ and *Terc*$^{+/-}$ backgrounds. Doxycycline (2 mg/ml in 5% sucrose) was administered in drinking water in light-protected bottles and changed biweekly. All mice were treated in accordance with AAALAC approved guidelines at Stanford University.

Northern blot, qRT-PCR, and telomerase activity analysis

Tissues were snap frozen in liquid nitrogen and then ground with mortar and pestle. RNA was isolated from organs by means of homogenization in Trizol. Five μg of total RNA was fractionated on a 0.8% formaldehyde gel, transferred to Hybond-N membrane (Amersham), and hybridized with TERT or GAPDH ^{32}P-labeled DNA probes. For qRT-PCR, 1 μg of total RNA was reverse transcribed, then subjected to qPCR using primer pairs specific for TERT, WT1, Axin2, Cyclin D2, Lef1, or HPRT1. SYBR-green analysis was performed using the 7900HT Fast Real-Time PCR System machine (ABI). The expression level of each gene was normalized to its corresponding HPRT1 level. For qRT-PCR on human samples, RNA was isolated from twenty 10μm cryosections using RNeasy Plus Micro kit (Qiagen), reverse transcribed, then subjected to qPCR using Taqman-based ABI gene expression assays. For telomerase repeat amplification protocol (TRAP) assays, protein was extracted from 50–100 μg of tissue in NP40 lysis buffer, and a TRAP reaction was performed (TRAPEZE, Chemicon).

Urine protein assays

Urine was collected from mice and assessed for protein content by SDS-PAGE followed by staining with Biosafe Coomassie blue (BioRad).

Histology

Kidneys were fixed overnight in 10% buffered formalin and embedded in paraffin. Five μm tissue sections were stained with hematoxylin and eosin (H&E) for microscopic analysis.

RNA in situ analysis

Digoxigenin-labeled RNA probes were synthesized *in vitro* using digoxigenin-UTP (Roche). In situ analysis was performed on 5 μm paraffin sections. Probes were detected using an alkaline phosphatase conjugated digoxigenin-specific antibody, developed using NBT/BCIP (Roche), and counterstained with nuclear fast red (Vector Laboratories).

Immunohistochemistry

Antigen retrieval was performed on 5 μm paraffin sections with Vector unmasking reagent (Vector Laboratories). Mouse monoclonal primary antibodies were detected using a biotinylated anti-mouse IgG (MOM, Vector Laboratories) followed by streptavidin-HRP, streptavidin-DyLight488 or streptavidin-Cy3 (Jackson ImmunoResearch). For immunostaining using rabbit and rat primary antibodies, kidney sections were blocked with PBS; 10g/L BSA; 5% NGS; 0.01% Triton, incubated with the primary antibody diluted in the blocking solution for overnight at 4°C, and detection was done with an HRP-, FITC- or DyLight549-conjugated anti-rabbit secondary antibody (Jackson ImmunoResearch). Primary

antibodies used were mouse monoclonal Ki-67-specifc (Pharmingen), rabbit monoclonal Ki-67-specific (Epitomics), mouse monoclonal synaptopodin-specific (Biodesign), rabbit monoclonal WT1-specific (Epitomics), rabbit VWF8-specific (Chemicon), rat BrdU-specific (BD), rabbit β-Galactosidase-specific (Coppel). For BrdU detection, slides were pre-treated in 1N HCl for 1hr at 37°C.

TUNEL analysis

TUNEL analysis was performed on 5 μm paraffin sections (Apoptag, Chemicon). Slides were deparaffinized, treated with proteinase K, quenched in 3% hydrogen peroxide, and incubated with terminal deoxynucleotidyl transferase to label apoptotic DNA with UTP-digoxigenin. Finally, sections were incubated with HRP-conjugated digoxigenin-specific antibody and visualized by chromogenic detection and hematoxylin counterstain.

Electron microscopy

Fresh kidney was diced with a razor blade into 1–2 mm^3 pieces, fixed with 3% glutaraldehyde and analyzed by electron microscopy using standard methods.

X-Gal whole mount staining

Axin2$^{lacz/+}$ reporter mice were intercrossed with i-TERT^{ci} mice and TERT was induced by administration of doxycycline as described above. After 14 days of doxycycline treatment, tissues were processed for X-gal staining. Tissues were fixed with 4% paraformaldehyde for 1 h at 4°C, washed 5 times for 30 min in wash buffer (2 mM $MgCl_2$, 0.01% deoxycholate, 0.02% NP-40 in PBS), then stained with X-gal solution (4 mM $K_3Fe(CN)_6$, 4mM $K_4Fe(CN)_6$, 20 mM Tris pH 7.4, 1 mg/mL X-gal in wash buffer) overnight at room temperature. The stained sample were washed, and post-fixed.

Survival Nephrectomy

Mice were anesthetized with ketamine/xylazine and the skin sterilized with betadine. A 2 cm dorsal midline skin incision was made with its cranial terminus at the level of the 13th rib. The abdominal wall was opened 1.5 to 2 cm lateral to the spine and the kidney was retracted through the incision. Renal blood vessels and the ureter were ligated with Ethilon 6-0 non-absorbable suture and the kidney removed. The muscle was approximated and the skin incision closed using vicryl 2-0 synthetic absorbable sutures.

Adenovirus Administration

Adult i-TERT^{ci} mice on doxycycline received a single intravenous tail vein injection of 3×10^8 plaque-forming units (pfu) of either Ad-Dkk1 or Ad-Fc. Five to 8 week old Tg26 mice received a single intravenous tail vein injection of 2.25×10^8 pfu of either Ad-Dkk1 or Ad-Fc.

Supplementary Material

Refer to Web version on PubMed Central for supplementary material.

Acknowledgments

We thank P. Chu in the Stanford Comparative Medicine Histology Research Core Laboratory, S. Busque for guidance with nephrectomy, and R. Nusse for *Axin2*$^{LacZ/+}$ mice. M. S. was supported by the Stanford School of Medicine Dean's postdoctoral fellowship and the Stanford Center on Longevity postdoctoral fellowship. This work was supported by grants DK085527 and DK085720 to C.J.K., DK087626 to A.G.G. and CA111691, CA125453 and AG033747 to S.E.A.

References

1. Nadasdy T, Laszik Z, Blick KE, Johnson LD, Silva FG. Proliferative activity of intrinsic cell populations in the normal human kidney. J Am Soc Nephrol. 1994; 4:2032–2039. [PubMed: 7919156]
2. Humphreys BD, et al. Intrinsic epithelial cells repair the kidney after injury. Cell Stem Cell. 2008; 2:284–291. [PubMed: 18371453]
3. Mundel P, Shankland SJ. Podocyte biology and response to injury. J Am Soc Nephrol. 2002; 13:3005–3015. [PubMed: 12444221]
4. Barisoni L, Kriz W, Mundel P, D'Agati V. The dysregulated podocyte phenotype: a novel concept in the pathogenesis of collapsing idiopathic focal segmental glomerulosclerosis and HIV-associated nephropathy. J Am Soc Nephrol. 1999; 10:51–61. [PubMed: 9890309]
5. Pavenstadt H, Kriz W, Kretzler M. Cell biology of the glomerular podocyte. Physiol Rev. 2003; 83:253–307. [PubMed: 12506131]
6. Kriz W. Podocyte is the major culprit accounting for the progression of chronic renal disease. Microsc Res Tech. 2002; 57:189–195. [PubMed: 12012382]
7. Welsh GI, et al. Insulin signaling to the glomerular podocyte is critical for normal kidney function. Cell Metab. 2010; 12:329–340. [PubMed: 20889126]
8. Pavenstadt H. Roles of the podocyte in glomerular function. Am J Physiol Renal Physiol. 2000; 278:F173–179. [PubMed: 10662721]
9. Kriz W. Progressive renal failure--inability of podocytes to replicate and the consequences for development of glomerulosclerosis. Nephrol Dial Transplant. 1996; 11:1738–1742. [PubMed: 8918614]
10. Shankland SJ, Wolf G. Cell cycle regulatory proteins in renal disease: role in hypertrophy, proliferation, and apoptosis. Am J Physiol Renal Physiol. 2000; 278:F515–529. [PubMed: 10751212]
11. Barisoni L, et al. Podocyte cell cycle regulation and proliferation in collapsing glomerulopathies. Kidney Int. 2000; 58:137–143. [PubMed: 10886558]
12. Husain M, D'Agati VD, He JC, Klotman ME, Klotman PE. HIV-1 Nef induces dedifferentiation of podocytes in vivo: a characteristic feature of HIVAN. AIDS. 2005; 19:1975–1980. [PubMed: 16260903]
13. Zuo Y, et al. HIV-1 genes vpr and nef synergistically damage podocytes, leading to glomerulosclerosis. J Am Soc Nephrol. 2006; 17:2832–2843. [PubMed: 16988066]
14. Rosenstiel P, Gharavi A, D'Agati V, Klotman P. Transgenic and infectious animal models of HIV-associated nephropathy. J Am Soc Nephrol. 2009; 20:2296–2304. [PubMed: 19497967]
15. Ding M, et al. Loss of the tumor suppressor Vhlh leads to upregulation of Cxcr4 and rapidly progressive glomerulonephritis in mice. Nat Med. 2006; 12:1081–1087. [PubMed: 16906157]
16. Korgaonkar SN, et al. HIV-1 upregulates VEGF in podocytes. J Am Soc Nephrol. 2008; 19:877–883. [PubMed: 18443354]
17. Ronconi E, et al. Regeneration of glomerular podocytes by human renal progenitors. J Am Soc Nephrol. 2009; 20:322–332. [PubMed: 19092120]
18. Appel D, et al. Recruitment of podocytes from glomerular parietal epithelial cells. J Am Soc Nephrol. 2009; 20:333–343. [PubMed: 19092119]
19. Lee HW, et al. Essential role of mouse telomerase in highly proliferative organs. Nature. 1998; 392:569–574. [PubMed: 9560153]

20. Allsopp RC, Morin GB, DePinho R, Harley CB, Weissman IL. Telomerase is required to slow telomere shortening and extend replicative lifespan of HSCs during serial transplantation. Blood. 2003; 102:517–520. [PubMed: 12663456]
21. Batista LF, et al. Telomere shortening and loss of self-renewal in dyskeratosis congenita induced pluripotent stem cells. Nature. 2011; 474:399–402. [PubMed: 21602826]
22. Sarin KY, et al. Conditional telomerase induction causes proliferation of hair follicle stem cells. Nature. 2005; 436:1048–1052. [PubMed: 16107853]
23. Choi J, et al. TERT promotes epithelial proliferation through transcriptional control of a Myc- and Wnt-related developmental program. PLoS Genet. 2008; 4:e10. [PubMed: 18208333]
24. Park JI, et al. Telomerase modulates Wnt signalling by association with target gene chromatin. Nature. 2009; 460:66–72. [PubMed: 19571879]
25. D'Agati V. Pathologic classification of focal segmental glomerulosclerosis. Semin Nephrol. 2003; 23:117–134. [PubMed: 12704572]
26. Imai E, et al. Glowing podocytes in living mouse: transgenic mouse carrying a podocyte-specific promoter. Exp Nephrol. 1999; 7:63–66. [PubMed: 9892816]
27. Kaplan JM, et al. Mutations in ACTN4, encoding alpha-actinin-4, cause familial focal segmental glomerulosclerosis. Nat Genet. 2000; 24:251–256. [PubMed: 10700177]
28. Marshall CB, Shankland SJ. Cell cycle regulatory proteins in podocyte health and disease. Nephron Exp Nephrol. 2007; 106:e51–59. [PubMed: 17570940]
29. Nagata M, Nakayama K, Terada Y, Hoshi S, Watanabe T. Cell cycle regulation and differentiation in the human podocyte lineage. Am J Pathol. 1998; 153:1511–1520. [PubMed: 9811343]
30. Mundel P, Reiser J, Kriz W. Induction of differentiation in cultured rat and human podocytes. J Am Soc Nephrol. 1997; 8:697–705. [PubMed: 9176839]
31. Mundel P, et al. Synaptopodin: an actin-associated protein in telencephalic dendrites and renal podocytes. J Cell Biol. 1997; 139:193–204. [PubMed: 9314539]
32. Reiser J, Kriz W, Kretzler M, Mundel P. The glomerular slit diaphragm is a modified adherens junction. J Am Soc Nephrol. 2000; 11:1–8. [PubMed: 10616834]
33. Heikkila E, et al. Densin and beta-catenin form a complex and co-localize in cultured podocyte cell junctions. Mol Cell Biochem. 2007; 305:9–18. [PubMed: 17581699]
34. Lustig B, et al. Negative feedback loop of Wnt signaling through upregulation of conductin/axin2 in colorectal and liver tumors. Mol Cell Biol. 2002; 22:1184–1193. [PubMed: 11809809]
35. Dickie P, et al. HIV-associated nephropathy in transgenic mice expressing HIV-1 genes. Virology. 1991; 185:109–119. [PubMed: 1926769]
36. Bruggeman LA, et al. Renal epithelium is a previously unrecognized site of HIV-1 infection. J Am Soc Nephrol. 2000; 11:2079–2087. [PubMed: 11053484]
37. Bafico A, Liu G, Yaniv A, Gazit A, Aaronson SA. Novel mechanism of Wnt signalling inhibition mediated by Dickkopf-1 interaction with LRP6/Arrow. Nat Cell Biol. 2001; 3:683–686. [PubMed: 11433302]
38. Mao B, et al. LDL-receptor-related protein 6 is a receptor for Dickkopf proteins. Nature. 2001; 411:321–325. [PubMed: 11357136]
39. Semenov MV, et al. Head inducer Dickkopf-1 is a ligand for Wnt coreceptor LRP6. Curr Biol. 2001; 11:951–961. [PubMed: 11448771]
40. Mao B, et al. Kremen proteins are Dickkopf receptors that regulate Wnt/beta-catenin signalling. Nature. 2002; 417:664–667. [PubMed: 12050670]
41. Kuhnert F, et al. Essential requirement for Wnt signaling in proliferation of adult small intestine and colon revealed by adenoviral expression of Dickkopf-1. Proc Natl Acad Sci U S A. 2004; 101:266–271. [PubMed: 14695885]
42. Iglesias DM, et al. Canonical WNT signaling during kidney development. Am J Physiol Renal Physiol. 2007; 293:F494–500. [PubMed: 17494089]
43. Stark K, Vainio S, Vassileva G, McMahon AP. Epithelial transformation of metanephric mesenchyme in the developing kidney regulated by Wnt-4. Nature. 1994; 372:679–683. [PubMed: 7990960]

44. Carroll TJ, Park JS, Hayashi S, Majumdar A, McMahon AP. Wnt9b plays a central role in the regulation of mesenchymal to epithelial transitions underlying organogenesis of the mammalian urogenital system. Dev Cell. 2005; 9:283–292. [PubMed: 16054034]

45. Lancaster MA, et al. Impaired Wnt-beta-catenin signaling disrupts adult renal homeostasis and leads to cystic kidney ciliopathy. Nat Med. 2009; 15:1046–1054. [PubMed: 19718039]

46. Lin SL, et al. Macrophage Wnt7b is critical for kidney repair and regeneration. Proc Natl Acad Sci U S A. 107:4194–4199. [PubMed: 20160075]

47. Dai C, et al. Wnt/beta-catenin signaling promotes podocyte dysfunction and albuminuria. J Am Soc Nephrol. 2009; 20:1997–2008. [PubMed: 19628668]

48. He W, Kang YS, Dai C, Liu Y. Blockade of Wnt/beta-catenin signaling by paricalcitol ameliorates proteinuria and kidney injury. Journal of the American Society of Nephrology : JASN. 2011; 22:90–103. [PubMed: 21030600]

49. Kato H, et al. The Wnt/{beta}-catenin pathway in podocytes integrates cell adhesion, differentiation and survival. J Biol Chem. 2011

50. Sagrinati C, et al. Isolation and characterization of multipotent progenitor cells from the Bowman's capsule of adult human kidneys. J Am Soc Nephrol. 2006; 17:2443–2456. [PubMed: 16885410]

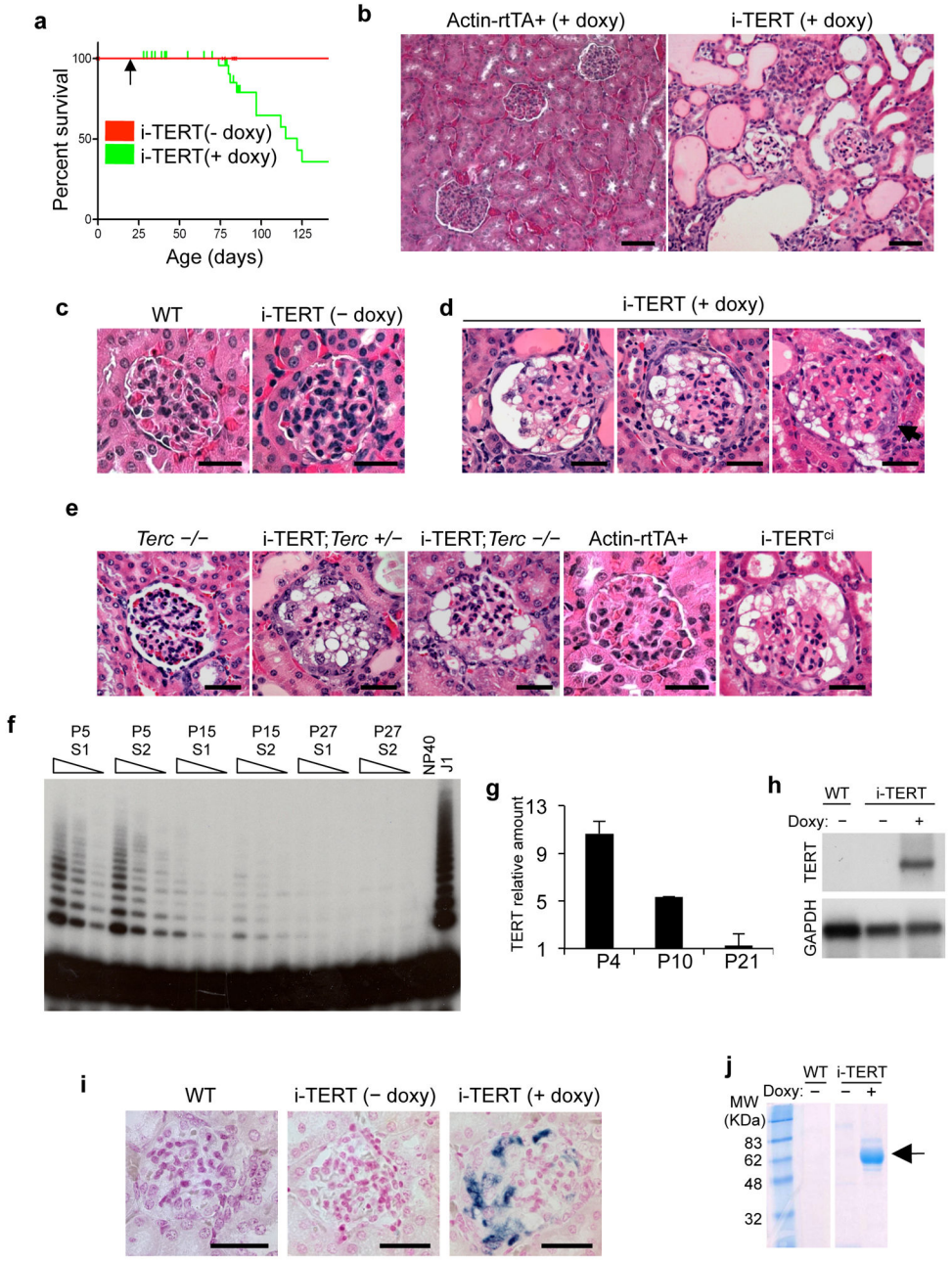

Figure 1.

Conditional induction of TERT impairs survival and induces a collapsing glomerulopathy. (**a**) Survival of i-TERT mice (− doxy, red; + doxy, green). Doxycycline (doxy) initiated at age 21 days (arrow). $P<0.001$ by Logrank test. (**b**) Kidney histology from Actin-rtTA+and i-TERT mice each on doxy for 44 days. H&E, scale bar = 50 μm. (**c–e**) Glomerular histology from: (**c**) wild-type mice (left panel) and i-TERT mice off doxy (right panel); (**d**) i-TERT mice on doxy for 44 days; (**e**) *Terc*$^{-/-}$, i-TERT;*Terc*$^{+/-}$ and i-TERT;*Terc*$^{-/-}$ mice on doxy for 56 days, and Actin-rtTA+ and i-TERT^{ci} mice each on doxy for 30 days. H&E, scale bar = 25 μm. (**f**) Telomerase activity by TRAP in wild-type whole mouse kidney at day 5 (P5),

day 15 (P15), and day 27 (P27) after birth. Two mice analyzed for each time point (S1 and S2). Range of concentrations represents two-fold serial dilutions of extract. Lysis buffer (NP40), negative control; mouse ES cells (J1), positive control. (**g**) TERT mRNA levels by qRT-PCR in whole mouse kidney at 4, 10, and 21 days of age. (**h**) Northern blot analysis for TERT mRNA in kidney from wild-type and i-TERT mice off (−) or on (+) doxy. (**i**) RNA in situ hybridization for TERT mRNA in wild-type and i-TERT mice off (−) or on (+) doxy. Scale bar = 25 μm. (**j**) Analysis of protein in urine by SDS-PAGE from wild-type (WT) or i-TERT mice off (−) or on (+) doxy.

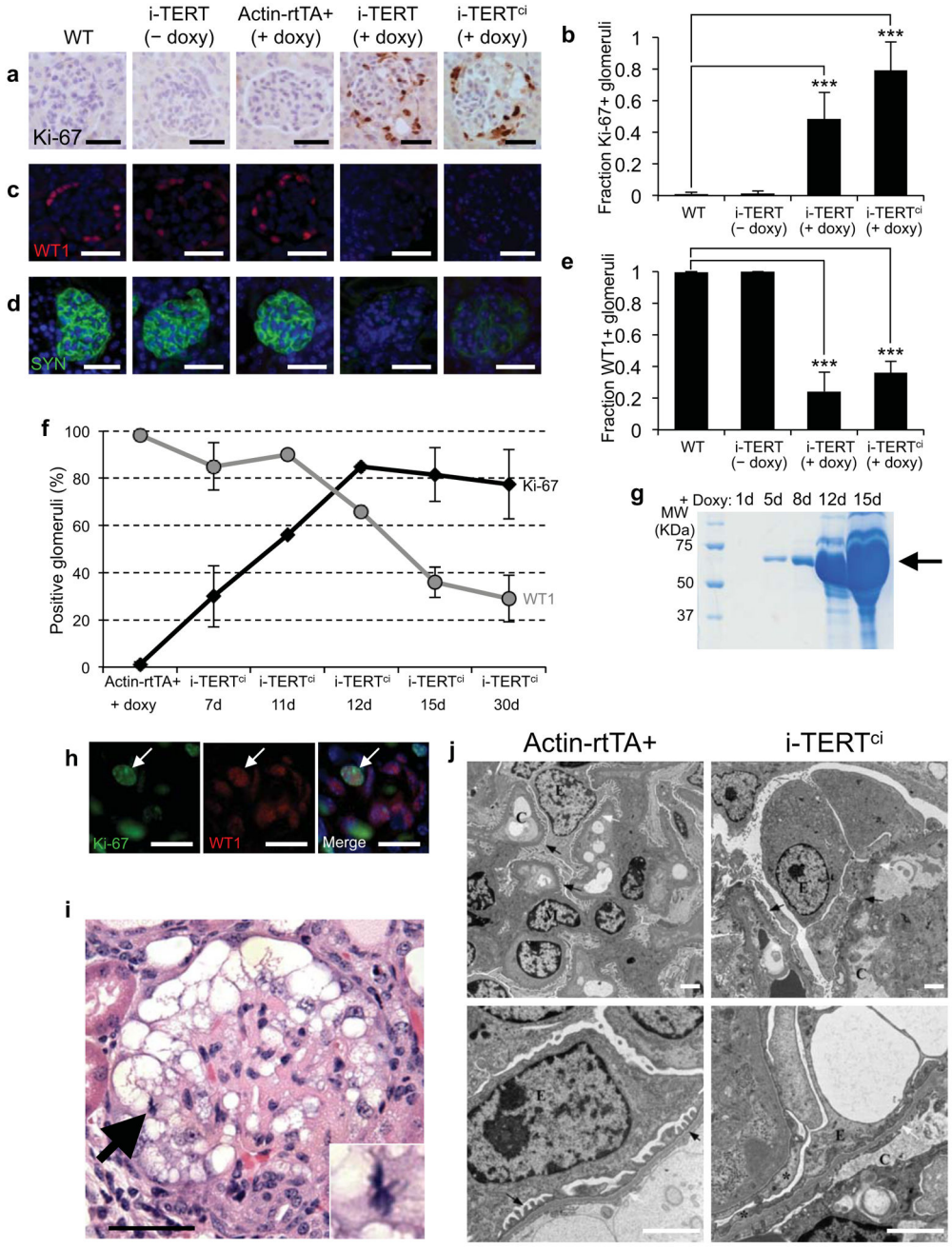

Figure 2.

TERT induces podocyte dedifferentiation and proliferation. (**a**) Ki-67 immunostaining in kidney sections from WT, i-TERT (− doxy), Actin-rtTA+ (+ doxy), i-TERT (+ doxy) and i-TERT^{ci} mice (+ doxy). Hematoxylin counterstain, scale bar = 25 μm. (**b**) Quantification of data in (a). Glomeruli harboring Ki-67 positive cells in WT (*n*=4), i-TERT (− doxy, *n*=3), i-TERT (+ doxy, *n*=3), and i-TERT^{ci} mice (+ doxy, *n*=3). ***P<0.0001, Fisher's exact test, i-TERT (+ doxy) or i-TERT^{ci} (+ doxy) versus WT. (**c–d**) Immunostaining for the podocyte-restricted markers, WT1 (**c**) and Synaptopodin (SYN) (**d**) in kidney sections from mice as in

(a), scale bar = 25 μm. (**e**) Quantification of data in (c). Fraction of glomeruli positive for WT1 in WT (*n*=2), i-TERT (− doxy, *n*=2), i-TERT(+ doxy, *n*=3) and i-TERT^{ci} mice (+ doxy, *n*=3). ***P<0.0001, Fisher's exact test, i-TERT (+ doxy) or i-TERT^{ci} (+ doxy) versus WT. (**f**) Percentage of glomeruli harboring Ki-67 positive cells (black) and WT1 positive cells (gray) in kidneys from Actin-rtTA+ control mice and i-TERT^{ci} mice treated with doxycycline (+ doxy) for 7, 11, 12, 15 or 30 days. (**g**) SDS-PAGE of urine collected from an i-TERT^{ci} mouse after 1, 5, 8, 12 and 15 days on doxy. (**h**) Double immunostaining for Ki-67 (green), and WT1 (red) in kidney sections from i-TERT^{ci} mice on doxy for 12 days, scale bar = 10 μm. (**i**) Mitotic figure in podocyte from i-TERT mouse on doxy for 44 days. H&E, scale bar = 25 μm. (**j**) Electron microscopy of glomeruli from Actin-rtTA+ (left panels) and i-TERT^{ci} (right panels) mice on doxy for 30 days. (C: capillary lumen, E: podocytes, M: mesangium, white arrows: glomerular basement membrane). Scale bar = 2 μm in all the panels.

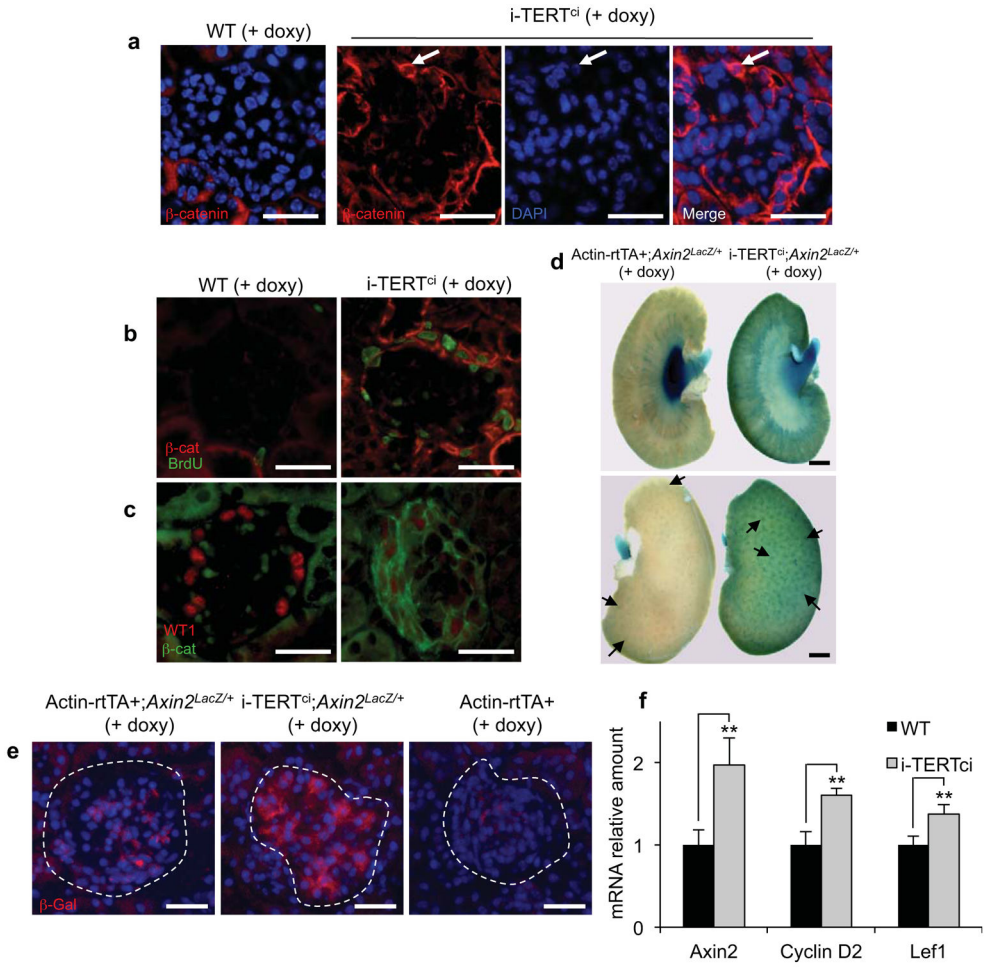

Figure 3.

TERT induces activation of the Wnt signaling pathway in podocytes. (**a**) Immunostaining for total β-catenin in kidney sections from WT and i-TERT^{ci} mice on doxy for 15 days. White arrow, nuclear β-catenin, scale bar = 25 μm. (**b**) Double immunostaining for BrdU (green), and β-catenin (β-cat, red) in kidney sections from WT and i-TERT^{ci} mice on doxy for 22 days and treated with BrdU drinking water for 8 days preceding sacrifice. Scale bar = 25 μm. (**c**) Double immunostaining for total β-catenin (β-cat, green), and WT1 (red) in kidney sections from WT and i-TERT^{ci} mice on doxy for 12 days, scale bar = 25 μm. (**d**) Whole-mount X-Gal staining of kidneys from Actin-rtTA+;*Axin2*$^{Laz/+}$ (left) and i-TERT^{ci};*Axin2*$^{LacZ/+}$ (right) mice treated with doxycycline for 13 days. Scale bar = 1 mm. (**e**) Immunostaining for β-Galactosidase (β-Gal) protein in kidney sections from Actin-rtTA +;*Axin2*$^{LacZ/+}$, i-TERT^{ci};*Axin2*$^{LacZ/+}$, and Actin-rtTA+ mice on doxy for 13 days. Scale bar = 25 μm. (**f**) Axin2, Cyclin D2, and Lef1 mRNA expression byqRT-PCR in whole kidneys from WT and i-TERT^{ci} mice on doxycycline treatment for 22 days. ***P*=0.0008, ***P*=0.0007, and ***P*=0.0005 by t-test for i-TERT^{ci} vs. WT mice for Axin2, CyclinD2 and Lef1, respectively.

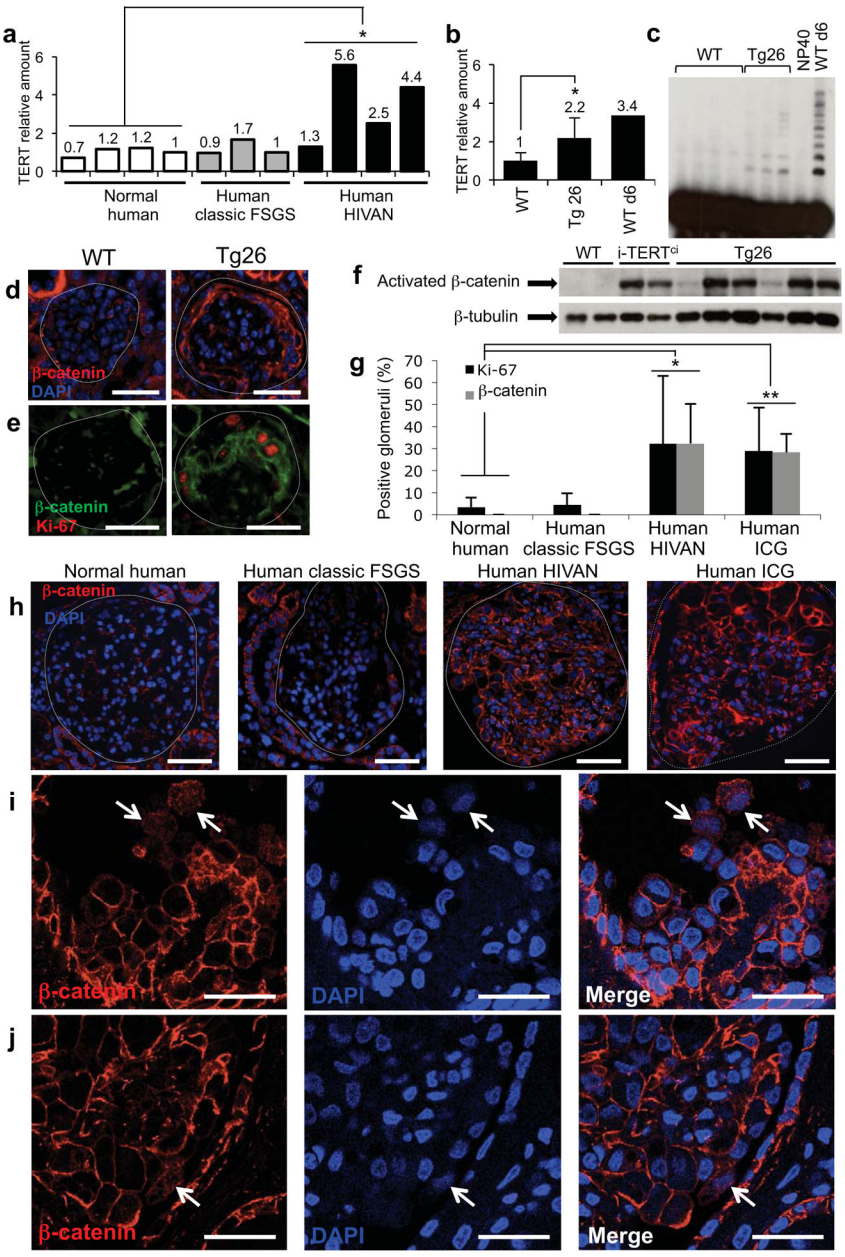

Figure 4.

β-catenin is stabilized and TERT expression is increased in human collapsing glomerulopathies and in a mouse model of HIVAN. (**a**) TERT mRNA levels by qRT-PCR in kidney biopsies from healthy individuals (*n*=4), and individuals with classic FSGS (*n=3*) or HIVAN (*n*=4). **P*=0.023, Student's t-test, HIVAN vs. normal. (**b**) TERT mRNA levels by qRT-PCR in whole kidneys from wild-type mice (*n=4*), Tg26 mice (*n=5*) and P6 wild-type mouse. **P*=0.021, t-test for Tg26 vs. wild-type. (**c**) Telomerase activity by TRAP in whole kidneys from 4 adult wild-type mice, and 3 adult Tg26 mice. NP40 buffer, negative control; WT d6 kidney, positive control. (**d, e**) Immunostaining in kidney sections from WT and HIV Tg26 mice for total β-catenin (d) and double immunostaining for the proliferation marker

Ki-67 (red), and β-catenin (green) (e). Scale bar = 25 μm. (**f**) Western blot for activated β-catenin in whole kidneys from adult WT mice (n=2), i-TERT^{ci} mice on doxy for 22 days (n=2), and Tg26 mice (n=6). (**g**) Percentage of glomeruli showing Ki-67 positive cells (black) and β-catenin stabilization (grey) in kidney sections from healthy individuals (*n*=7), and individuals with classic FSGS (*n=8*), HIVAN (*n*=5), or ICG (*n*=5). **P*=0.004, t-test for normal vs. HIVAN; **P*=0.0001, normal vs. ICG. (**h**) Immunostaining for total β-catenin (red) in kidney sections from healthy individuals, and individuals with classic FSGS, HIVAN or ICG. Scale bar = 50 μm. (**i–j**) Immunostaining for totalβ-catenin by confocal microscopy in HIVAN (i) and ICG (j) kidney sections. White arrows, nuclear and cytoplasmicβ-catenin. Scale bar = 25 μm.

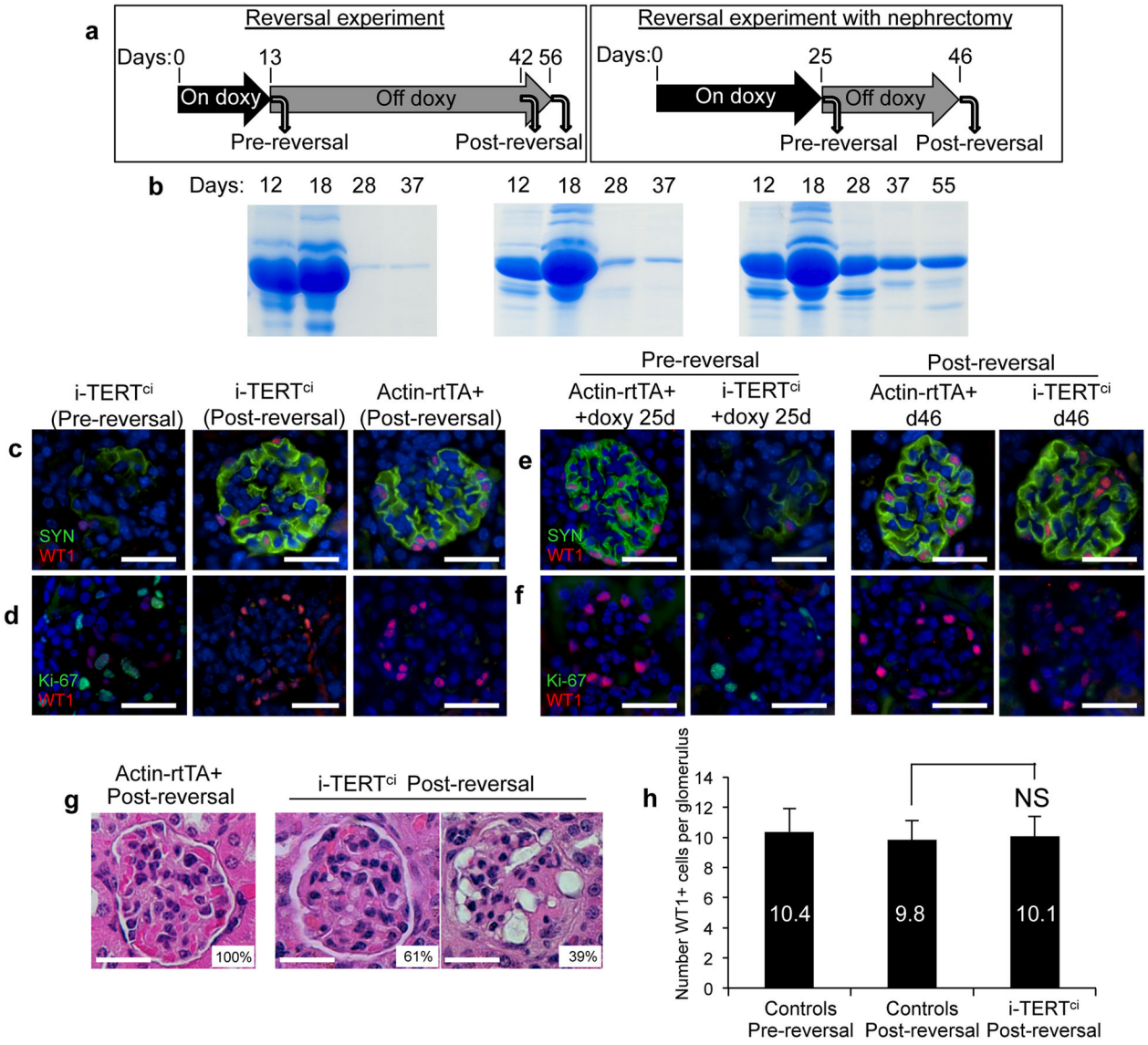

Figure 5.

Proliferating podocytes return to a quiescent, differentiated state after doxycycline withdrawal in i-TERT^{ci} mice. (**a**) For TERT reversal experiment (left), 6 i-TERT^{ci} mice were treated with doxy, three mice were sacrificed at day 13 (Pre-reversal) and doxy was removed from the remaining three mice, which were aged until at least 42 days (Post-reversal). For reversal with nephrectomy (right), two Actin-rtTA+ and two i-TERT^{ci} mice were treated with doxycycline. Each mouse underwent survival nephrectomy at day 25, doxy was withdrawn after surgery and the mice were aged until day 46. (**b–d**) Reversal experiment. (**b**) Serial analysis of protein in urine by SDS-PAGE in three i-TERT^{ci} mice treated with doxy as described in (a, left). (**c, d**) Double immunostaining for synaptopodin (SYN, green) and WT1 (red) (**c**) or for Ki-67 (green) and WT1 (red) (**d**) in kidney sections from i-TERT^{ci} mice on doxy for 13 days (+ doxy), and i-TERT^{ci} or Actin-rtTA+ mice on doxy for 13 days then reversed for 29 days. Scale bar = 25 μm. (**e–g**) Reversal experiment

with nephrectomy. (**e,f**) Double immunostaining for synaptopodin (SYN, green) and WT1 (red) (**e**) or for Ki-67 (green) and WT1 (red) (**f**) in kidney sections from nephrectomized i-TERT^{ci} and Actin-rtTA+ control mice, as described in (a, right). Scale bar = 25 μm. (**g**) H&E stained sections of post-reversal kidney from nephrectomized i-TERT^{ci} or Actin-rtTA + mice at day 46. Percentage of glomeruli showing a morphology similar to that outlined is indicated. Scale bar = 25 μm. (**h**) Quantification of podocyte density in glomeruli of control mice pre- and post-reversal, and in glomeruli of i-TERT^{ci} mice after reversal. NS, not significant. P=0.39, t-test for i-TERT^{ci} post-reversal vs. controls post-reversal.

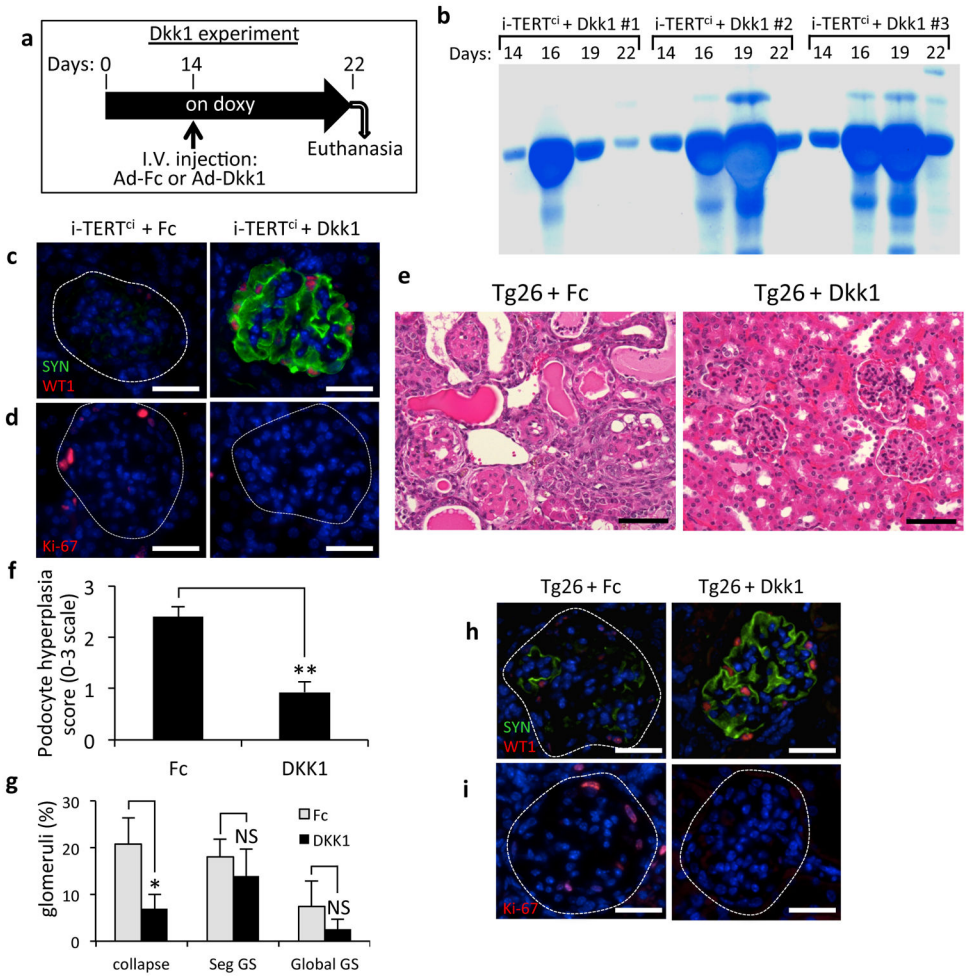

Figure 6.

Acute inhibition of Wnt signaling in i-TERT^{ci} and Tg26 HIVAN mice ameliorates disease progression. (**a**) Schematic of Dkk1 experiment in i-TERT^{ci} mice. Five i-TERT^{ci} mice were treated with doxycycline for 22 days. Fourteen days after the start of doxy, mice were injected with Ad-Fc (n=2) or with Ad-Dkk1 (n=3), then sacrificed at day 22. (**b**) Serial analysis of protein in urine by SDS-PAGE in three i-TERT^{ci} mice injected with Ad-Dkk1. (**c–d**) Double immunostaining for synaptopodin (SYN, green) and WT1 (red) (**c**) and single immunostaining for Ki-67 (red) (**d**) in kidney sections from i-TERT^{ci} mice injected with either Ad-Fc or Ad-Dkk1. Scale bar = 25 μm. (**e**) Kidney histology from Tg26 mice injected with either Ad-Fc (left) or Ad-Dkk1 (right). H&E, scale bar = 50 μm. (**f**) Histological assessment of podocyte hyperplasia in Ad-Fc and Ad-Dkk1 Tg26 groups graded on a semi-quantitative scale of 0–3 based on the degree of podocyte hyperplasia in individual affected glomeruli and the number of glomeruli with this finding within a sample. ***P*=0.0008, t-test for Ad-Dkk1 vs. Ad-Fc. (**g**) Scoring of kidney histology in Ad-Fc and Ad-Dkk1 Tg26 groups for collapsed glomeruli (collapse), segmental glomerulosclerosis (Seg GS) or global glomerulosclerosis (Global GS), in blinded analysis of 100 glomeruli per section. **P*=0.02, *P*=0.3 and *P*=0.2 respectively by t-test for Ad-Dkk1 vs. Ad-Fc. NS, not significant. (**h,i**) Double immunostaining for synaptopodin (SYN, green) and WT1 (red) (**h**) and single

immunostaining for Ki-67 (red) (**i**) in kidney sections from Tg26 mice injected with either Ad-Fc or Ad-Dkk1. Scale bar = 25 μm.